

Suppression of ferromagnetism and metal-like conductivity in lightly Fe-doped SrRuO₃

Jiyu Fan, Sicheng Liao, Wenqin Wang, Lei Zhang, Wei Tong et al.

Citation: *J. Appl. Phys.* **110**, 043907 (2011); doi: 10.1063/1.3624764

View online: <http://dx.doi.org/10.1063/1.3624764>

View Table of Contents: <http://jap.aip.org/resource/1/JAPIAU/v110/i4>

Published by the [American Institute of Physics](#).

Related Articles

Thickness effects on the magnetic and electrical transport properties of highly epitaxial LaBaCo₂O_{5.5+δ} thin films on MgO substrates

Appl. Phys. Lett. **101**, 021602 (2012)

Tailoring coercivity of unbiased exchange-coupled ferromagnet/antiferromagnet bilayers

J. Appl. Phys. **112**, 013904 (2012)

Magnetoresistance and magnetocaloric properties involving strong metamagnetic behavior in Fe-doped Ni₄₅(Co_{1-x}Fe_x)₅Mn_{36.6}In_{13.4} alloys

Appl. Phys. Lett. **101**, 012401 (2012)

Mean field renormalization group: A theoretical approach to the Fe^{1-q}Al^q in the bcc lattice

J. Appl. Phys. **111**, 113921 (2012)

Study on spin-splitting phenomena in the band structure of GdN

Appl. Phys. Lett. **100**, 232410 (2012)

Additional information on J. Appl. Phys.


Journal Homepage: <http://jap.aip.org/>

Journal Information: http://jap.aip.org/about/about_the_journal

Top downloads: http://jap.aip.org/features/most_downloaded

Information for Authors: <http://jap.aip.org/authors>

ADVERTISEMENT



Special Topic Section:
PHYSICS OF CANCER

Why cancer? Why physics? [View Articles Now](#)

Suppression of ferromagnetism and metal-like conductivity in lightly Fe-doped SrRuO₃

Jiyu Fan,^{1,a)} Sicheng Liao,² Wenqin Wang,² Lei Zhang,³ Wei Tong,³ Langsheng Ling,³ Bo Hong,⁴ Yangguang Shi,¹ Yan Zhu,¹ Dazhi Hu,¹ Li Pi,^{2,3} and Yuheng Zhang^{2,3}

¹Department of Applied Physics, Nanjing University of Aeronautics and Astronautics, Nanjing 210016, China

²Hefei National Laboratory for Physical Sciences at the Microscale, University of Science and Technology of China, Hefei 230026, China

³High Magnetic Field Laboratory, Chinese Academy of Sciences, Hefei 230031, China

⁴Department of Material Engineering, China Jiliang University, Hangzhou 310018, China

(Received 27 May 2011; accepted 12 July 2011; published online 18 August 2011)

The magnetic and electronic transport properties of the lightly doped SrRu_{1-x}Fe_xO₃ ($x \leq 0.15$) have been studied. All the samples show a paramagnetic-ferromagnetic phase transition and hysteresis effect. With the increase of Fe, the temperature of magnetic phase transition decreases but coercive field increases indicating the existence of antiferromagnetic interaction and magnetic-crystalline anisotropy. In low temperature, all the doping samples exhibit an insulating behavior while metal feature appears only at $x \leq 0.10$ samples. The induced disorder suppresses the itinerant property of Ru 4d electron due to Fe random occupation. As a result, the ferromagnetism is weakened and metal-insulator transition is suppressed. © 2011 American Institute of Physics. [doi:10.1063/1.3624764]

I. INTRODUCTION

Over the past few years, the electronic and magnetic properties of 4d perovskite-type ruthenium oxides have been paid a significant attention, both from a fundamental science point-of-view, but increasingly due to their actual and potential application.¹⁻³ The Ruddlesden-Popper Sr-based ruthenates,⁴ Sr_{n+1}Ru_nO_{3n+1}, exhibit the variable properties with different n . As $n = 1$, Sr₂RuO₄ is a p-wave spin-triplet superconductivity.^{5,6} For $n = 2$, Sr₃Ru₂O₇ is a metal with a metamagnetic quantum critical end point.^{7,8} For $n = \infty$, SrRuO₃ is an itinerant ferromagnetic (FM) metal with Curie temperature around $T_C = 161$ K.^{1,9} The FM behavior of SrRuO₃ has been attributed to the highly correlated Ru 4d-electron band where the low spin Ru⁴⁺ ions have localized 4d electrons with magnetic moments from 0.8 to 1.6 μ_B /Ru.^{10,11} The magnetic critical behavior of SrRuO₃ agrees with the conventional 3D Ising model and is consistent with the experimentally observed uniaxial anisotropy in the system.¹²

At present, to further investigate and clarify the peculiar properties of SrRuO₃, the chemical substitutions with different elements for Ru⁴⁺ ions have been extensively adopted. According to ions with or without magnetic moment, the chemical substitutions can be classified into two groups, one is nonmagnetic doping pattern, such as Ti⁴⁺, Pb⁴⁺, Zn²⁺, Mg²⁺,¹³⁻¹⁶ the other is magnetic doping pattern, such as Cr³⁺, Mn³⁺, Co²⁺, Ni²⁺, Cu²⁺.^{13,17,18} Generally, as for the former dopant, the nonmagnetic ions directly disrupt the coupling of 4d-orbital of Ru⁴⁺ to the 2p-orbital of O²⁻ which is responsible for the ferromagnetic metal of SrRuO₃. Therefore, most of samples with non-magnetic dopant exhibit an insulated behavior even for very low doping concentration implying that the Ru-O sublattices are sensitive to the change

of local environment. On the other hand, as for the latter doping pattern, the complex magnetic phase transition frequently appears due to extra magnetic interaction between magnetic dopant and Ru⁴⁺ ions. Furthermore, the magnetic dopants can remarkably decrease the FM Curie temperature, except for Cr.¹⁸ Fe element, being one of main transitional metals, its substitution for Ru⁴⁺ has also been investigated previously.¹⁹⁻²¹ Bansal *et al.* reported that the substitution with Fe transforms SrRuO₃ into a paramagnetic (PM) and insulating state.¹⁹ Moreover, as the Fe concentration $x \geq 0.26$, the system shows an insulating behavior in the whole temperature range. Mamchik *et al.* proposed that the magnetic coupling between the high spin Fe³⁺ and low spin Ru⁴⁺ is FM interaction due to a large negative magnetoresistance observed in solid solution (SrRu)_{1-x}(LaFe)_xO₃.²⁰ In addition, a spin glass behavior has been reported in SrRu_{0.5}Fe_{0.5}O₃ by Nomura *et al.*²¹ Many experimental results from the measurement of Mössbauer spectra have confirmed that the dopant Fe existed as trivalent Fe³⁺ ion with a high spin state $t_{2g} \uparrow^3 e_g \uparrow^2$ ($S = \frac{5}{2}$) in the SrRu_{1-x}Fe_xO₃.^{19,21} In view of the great sensibility of Ru-O sublattices and a large spin magnetic moment of Fe³⁺ ion, we think the substitution of Ru⁴⁺ ions with the low concentration Fe³⁺ ions is better to study the magnetic transformation. Therefore, in this paper, we focus on the investigation of lightly doped SrRu_{1-x}Fe_xO₃ ($0 \leq x \leq 0.15$). All samples show a PM-FM phase transition and a large hysteresis loop. However, with the increase of Fe, the ferromagnetism was suppressed implying the antiferromagnetic (AFM) appearance. As $T < 100$ K, all doping samples exhibit an insulating behavior while the metal property only occurs at $T > 250$ K and $T > 100$ K for $x = 0.10$ and $x = 0.05$, respectively. The Fe random occupation causes a large disorder effect which weakens systematic ferromagnetism and electronic conductivity in the doped materials.

^{a)}Electronic mail: fanjiyu@gmail.com. Tel: +86-25-52075729. FAX: 86-25-83336919.

II. EXPERIMENT

Polycrystalline $\text{SrRu}_{1-x}\text{Fe}_x\text{O}_3$ samples ($0.00 \leq x \leq 0.15$) were prepared by traditional solid-state reaction method.²² The structure and phase purity of as-prepared samples were checked by powder x-ray diffraction (XRD) using Cu K_α radiation at room temperature. As shown in Fig. 1, the XRD patterns proved that all samples were in a single crystallographic phase of orthorhombic structure and space group of Pnma, in agreement with the previous structural study with x-ray and neutron diffraction.²³ The refined cell parameters and the corresponding cell volumes are listed in Table I. Obviously, with the increase of Fe, both of the lattice parameter “a” and cell volume “V” decrease. Magnetic measurements were performed by using a SQUID magnetometer (Quantum Design MPMS). The resistivity measurement were performed by the conventional four-probe method.

III. RESULTS AND DISCUSSION

Figure 2 shows the temperature dependence of magnetization (M - T) of $\text{SrRu}_{1-x}\text{Fe}_x\text{O}_3$ ($0.00 \leq x \leq 0.15$) measured in the magnetic field of 100 Oe. All data were taken in the warming run after zero-field cooling (ZFC, solid circle) and field cooling (FC, solid rectangle), respectively. In Fig. 2(a), the parent sample SrRuO_3 exhibits a sharp PM-FM phase transition. The Curie temperature (T_C), defined by the minimum in dM/dT , has been determined to be $T_C = 160.1$ K, which is much consistent with the previous reports indicating that the present sample is of high quality.^{10,11} With the increase of Fe, as shown in the magnified inset of Fig. 2, the temperature of maximal magnetization (T_M) was shifted from $T_M = 151$ K for $x = 0.05$ to $T_M = 114$ K for $x = 0.15$. Obviously, in low temperature, all sample’s ZFC and FC curves exhibit a considerable divergence about with 10 order of magnitude, similar to a metamagnetic behavior. The properties have been also observed in other doping SrRuO_3 compounds and generally attributed to spin glass state. However, the recent experiment of ac magnetization measured with different frequency did not provide any evidence of spin glass state due to spin frustration effect.^{24,25} On the contrary, more and more experimental evidences reveal that the peak of maximal magnetization of the ZFC curve gradually superposes that of

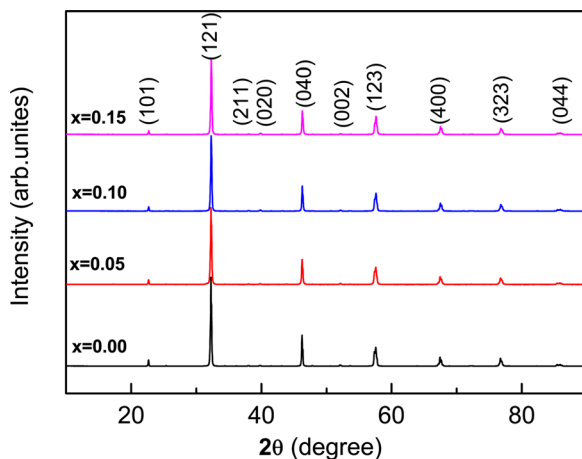


FIG. 1. (Color online) The x-ray diffraction patterns of the $\text{SrRu}_{1-x}\text{Fe}_x\text{O}_3$ ($0.00 \leq x \leq 0.15$).

TABLE I. Refined unit cell parameters and cell volume for $\text{SrRu}_{1-x}\text{Fe}_x\text{O}_3$ assuming Pnma space group.

Composition (x)	A (Å)	b (Å)	c (Å)	V (Å ³)
0.00	5.702	7.846	5.521	247.034
0.05	5.549	7.843	5.538	241.068
0.10	5.544	7.840	5.534	240.585
0.15	5.529	7.840	5.533	239.876

FC curve with the increase of dopant. Therefore, the reasonable interpretation should be large magnetic anisotropy in the domain region in low doped samples. In fact, as explained in the following section, a large coercivity field, which strong correlates with the magnetic anisotropy, has been even observed in the undoped SrRuO_3 .

Due to the application of the low doped pattern, the process of magnetic variation can be clearly revealed in the inset of Fig. 2. As $0.05 \leq x \leq 0.10$, below the Curie temperature, the magnetization undergoes two transformations. It first decreases and then reaches a terrace. After that, it continues to decrease until to the lowest temperature. However, as for $x = 0.15$ sample, one can only observed one transformation process. Notably, in low temperature, the rapid decrease of magnetization implies the suppression of FM coupling and the increase of antiferromagnetic coupling. The variation can be understood from two aspects. First, with the increase of Fe content, the Ru 4d bandwidth is narrowed due to the dilution of Ru^{4+} ions so that ferromagnetism is suppressed. Secondly, as mentioned in the former introduction, Fe ions exist as the trivalent Fe^{3+} ions when they substitute Ru^{4+} ions. In order to balance the valent in the system, some Ru^{4+} ions were transformed into Ru^{5+} ions. Therefore, the reascent magnetic interactions between Ru^{4+} , Ru^{5+} , and Fe^{3+} ions inevitably compete with the intrinsic FM coupling of Ru^{4+} - Ru^{4+} . Thus, it is possible to present some antiferromagnetism and even some local magnetic phase separation which results in the decrease of magnetization. In order to further clarify the reason, we used the Cuire-Weiss formula to analyze the χ^{-1} versus T curve which has been plotted in Fig. 3.

$$\chi = \frac{C}{T - \theta}, \quad (1)$$

where $c = N_A \mu_B^2 P^2 / 3k_B$ is the Curie constant, N_A is Avogadro constant, μ_B is the Bohr magneton, $P = g \sqrt{S(S+1)}$ is the effective magnetic moment, $g = 2$ is the gyromagnetic ratio and S is the magnetic spin, k_B is Boltzmann constant, θ is paramagnetic Weiss temperature. The fitting parameters (P_{exp} and θ) obtained from Eq. (1) are summarized in Table II. With increase of Fe, the effective magnetic moment and Weiss temperature slowly decrease. These parameters are consistent with the suppression of magnetization and the decrease of Curie temperature. According to the requirement of chemical valent compensation, the substitution for one Ru^{4+} ion will correspond to the appearance of one Ru^{5+} ion. The effective magnetic moment of Fe^{3+} and Ru^{5+} ions are $5.9 \mu_B$ and $3.87 \mu_B$, respectively. Both of them are larger than that of Ru^{4+} ions ($2.83 \mu_B$). Therefore, according to the general Eq. (2), the calculated effective magnetic moment

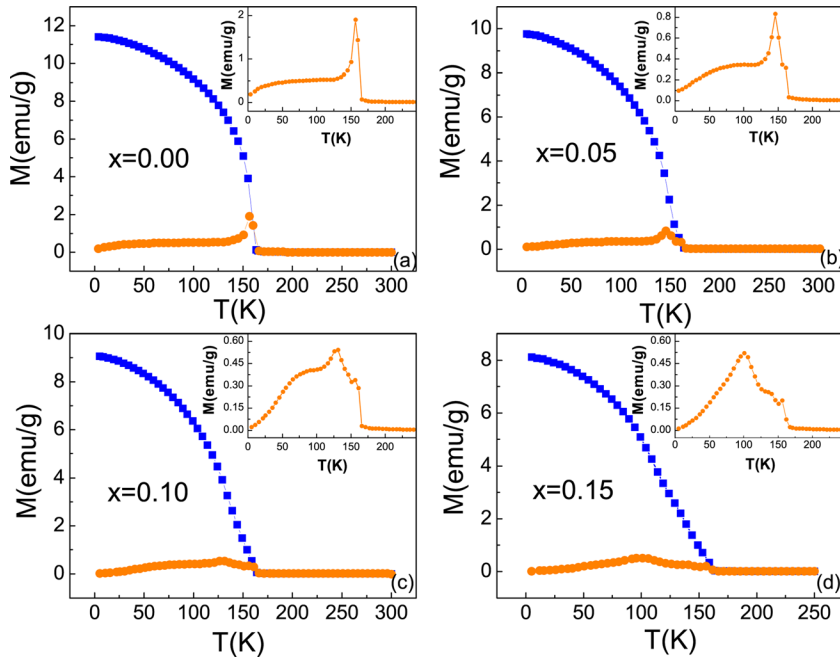


FIG. 2. (Color online) Temperature dependence of magnetization measured at $H = 100$ Oe (solid circle for ZFC, solid rectangle for FC). Inset shows the magnified ZFC curve.

(P_{cal}) of $\text{SrRu}_{1-x}\text{Fe}_x\text{O}_3$ would increase with Fe concentration contrary to the experimental measurement (see Table II).

$$P_{cal} = \sqrt{(1-2x)P_{\text{Ru}^{4+}}^2 + x(P_{\text{Fe}^{3+}}^2 + P_{\text{Ru}^{5+}}^2)}. \quad (2)$$

In the current material, we used the Fe^{3+} ions to substitute Ru^{4+} ions in SrRuO_3 . Generally, we always think that the Fe^{3+} ions should occupy on the positions of Ru^{4+} ions. However, Felner *et al.* recently found the Fe ions preferred to reside in the Sr site rather than Ru site as they investigated the Fe-doped powder SrRuO_3 and $\text{Sr}_{1-x}\text{Cu}_x\text{RuO}_3$.²⁶ Therefore, based on their experimental evidences, we change the above Eq. (2) to recalculate the effective magnetic moment. Here, we first assume all of Fe^{3+} ions occupy in Sr site. Moreover, the magnetic interaction between A-site (Fe^{3+})

and B-site (Ru^{4+}) can be considered to be FM due to the shorter distance of Sr-Ru comparison with that of Ru-Ru while the magnetic interaction between Ru^{4+} and Ru^{5+} shows as AFM.^{20,27} Thus, the Eq. (2) can be rewritten as

$$P'_{cal} = \sqrt{(1-2x)P_{\text{Ru}^{4+}}^2 + x(P_{\text{Fe}^{3+}}^2 - P_{\text{Ru}^{5+}}^2)}. \quad (3)$$

Obviously, as shown in Table II, the new calculated effective magnetic moment P'_{cal} is very close to the experimental values of P_{exp} . However, there are a little bit discrepancy between the P'_{cal} and P_{exp} indicating that the Fe ions only partly occupy in Sr site. In order to obtain the ratio of Fe in Sr-site, we introduce a parameter (A) into Eq. (3). A represents the Fe-probability in Sr site while (1-A) represents the Fe-probability in Ru site. The calculated results shows the Fe-occupancy in Sr site changes from $A = 91.7\%$ for $x = 0.05$ down to 89% for $x = 0.15$ in good agreement with results in Ref. 26. Therefore, the decrease of Fe-occupancy in Sr site causes the decrease of ferromagnetism in the highest doped $x = 0.15$ sample. Moreover, the AFM interaction between Fe^{3+} and Ru^{4+} also decreases the effective magnetic moment. With decrease of temperature and increase of Fe concentration, these AFM clusters grow in size and their interactions become stronger. Therefore, a consecutive reduction of ferromagnetism and the temperature of phase transition has been observed in the present samples.

Here, in order to understand the role of AFM phase occurred in the Fe doped SrRuO_3 , the M-H high field loop has been measured at special temperatures and the results have been shown in Fig. 4. All the doped samples display a noticeable magnetic hysteresis, indicating a cooperative behavior and a kind of ordered state. However, we can notice, in the lowest temperature ($T = 4.0$ K) and under the highest magnetic field ($H = 6.0$ T), the magnetization does not reach saturation indicating a large degree of the spin disorder with a high magnetic anisotropy. Chakravarti *et al.* has

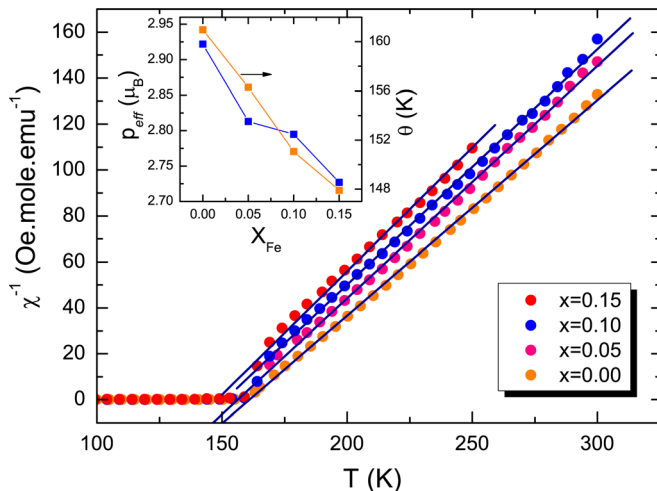


FIG. 3. (Color online) Inverse susceptibility vs temperature for all samples (solid circle); the straight line is the fitting results by using Curie-Weiss equation. The inset shows the effective magnetic moment and Weiss temperature vs the Fe concentration.

TABLE II. Some related parameters of SrRu_{1-x}Fe_xO₃ (see text for details).

Composition (<i>x</i>)	T_M (K)	θ (K)	$P_{exp}(\mu_B)$	$P_{cal}(\mu_B)$	$P'_{cal}(\mu_B)$	A(%)	$M_S(\mu_B)$	H_c (KOe)
0.00	156.4	160.91	2.922	2.83	2.83	0	1.58	2.0
0.05	151	156.29	2.813	3.114	2.864	91.7	1.021	3.2
0.10	131	151.08	2.795	3.374	2.897	91.6	1.007	3.8
0.15	114	147.91	2.727	3.616	2.929	89	0.992	4.5

previously pointed out the phenomenon stems from the external magnetic field which is not high enough to align all the spins in the direction of the applied magnetic field.²⁸ In fact, the degree of spin disorder is strongly correlated to the coercive field H_c . The larger coercivity means the higher disorder of spin. As shown in Fig. 4(d), the value of coercive field H_c increases from 2.0 KOe for SrRuO₃ to the 4.5 KOe for SrRu_{0.85}Fe_{0.15}O₃, implying a highest disorder of spin in the SrRu_{0.85}Fe_{0.15}O₃. Therefore, the Fe³⁺ random occupation suppresses the hybridization of Ru⁴⁺ - O²⁺ and induces a considerable disorder in the materials. Moreover, as seen from Table II, one can find the saturated magnetization (M_S), deduced by the extrapolation of M-H curves ($H=0$), exhibits a decrease similar to the variation of the effective magnetic moment and Weiss temperature. Therefore, the substitutions of Ru⁴⁺ with Fe³⁺ not only weaken the ferromagnetism but also induce more disorder and a larger magnetic anisotropy. These variations necessarily affect the electronic transport in the doped materials.

SrRuO₃ is well known for metallic electronic transport. As shown in Fig. 5(a), a consecutive decrease of resistivity with temperature has been observed and an obvious drop occurs at $T_C = 161$ K due to the reduced spin-disordered scattering.²⁹ Theoretically, the metallic property of SrRuO₃ can be understood with the Mott-Hubbard model since for its large bandwidth

(W) and a small intra-atomic Coulomb repulsion (U) which gives rise to the ratio $W/U \gg 1$. However, as the carrier mean free path shortens to the extent that can be comparable with the lattice constant, a very small disorder can cause a large variation for electronic conductivity. From Figs. 5(b), 5(c), and 5(d), one can find all doped samples exhibit an insulator rather than metallic feature in low temperatures. Moreover, the residual resistivities increase from sample of $x=0.05$ to $x=0.15$. As for the $x=0.05$ and $x=0.10$ samples, we can clearly observe that the resistivity minimum increases from 0.0145 to 0.0152 Ω cm and shifts to higher temperature from 100.7 to 238.9 K. Therefore, with increase of Fe concentration, the electronic conductivity has been modified remarkably. Compare the resistivity variation with the magnetization change as shown in M-T curves, we can find the latter behavior does not exhibit a large change as the Fe concentrations are increased to $x=0.15$. In fact, the granular nature is a general property in the polycrystalline samples. The appearance of grain boundaries can remarkably affect the magnitude of resistivity but without affecting the magnetic behavior. In the present sample, the competitions between the AFM phase and the FM phase intensify the grain boundaries in the low temperature. Therefore, below 100 K, a rapid rise of resistivity can be reflected from ρ - T curves. Moreover, the Fe random occupation induces disorder which weakens the itinerant property of Ru 4d electron and causes the carrier localization. Thus,

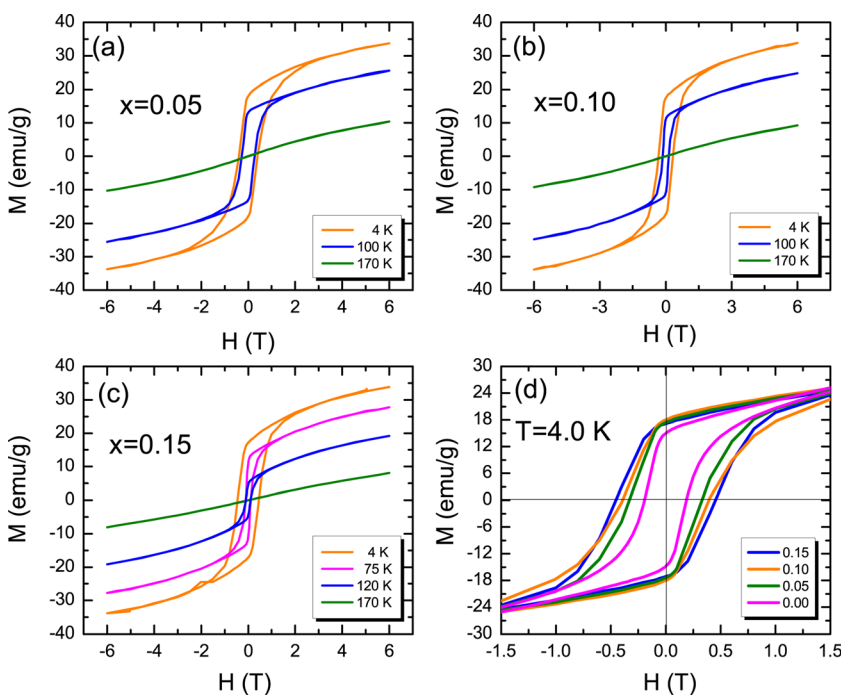


FIG. 4. (Color online) Isothermal magnetization measured at different temperatures for all doped samples; the fourth plot is the magnified loop for all samples.

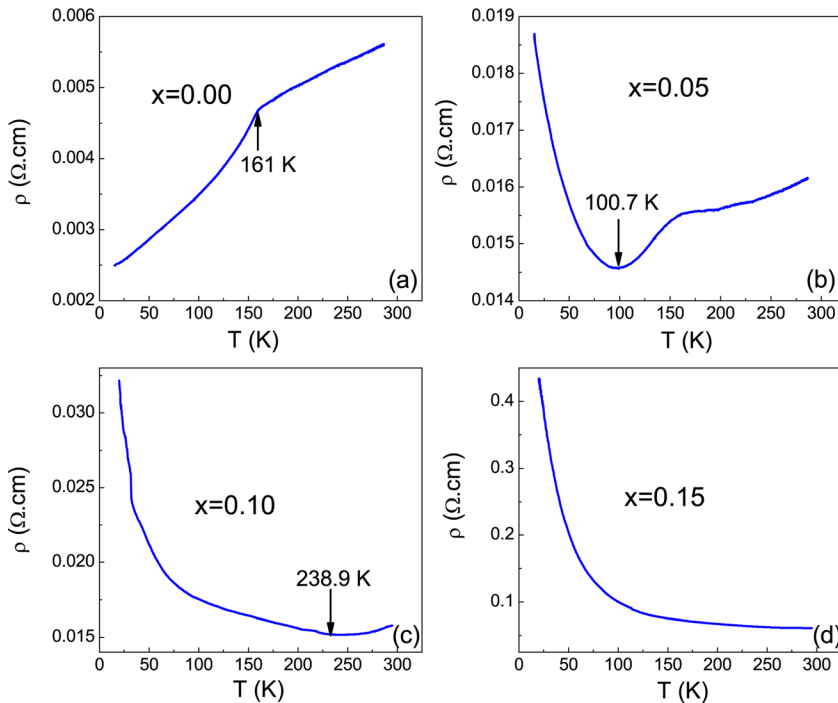


FIG. 5. (Color online) Temperature dependence of resistivity for samples with different compositions.

all the doped materials show an insulating behavior in low temperatures.

IV. CONCLUSION

In summary, we have investigated the magnetic and electronic transport properties of the low-doped $\text{SrRu}_{1-x}\text{Fe}_x\text{O}_3$ ($0 \leq x \leq 0.15$). The Fe dopants weaken the itinerant property of Ru 4d electron and induce a large disorder which is responsible for the decrease of ferromagnetism and the increase of magnetic crystalline anisotropy. In addition, the Fe random occupation results in the carriers localization and the insulating behavior in low temperatures.

ACKNOWLEDGMENTS

This work was supported by NUA Research Funding (No. NS2010187) and the National Nature Science Foundation of China (Grant Nos. 10904149, 10334090, 11004196, 11004194, and 51001061).

¹Y. Maeno, H. Hashimoto, K. Yoshida, S. Nishizaki, T. Fujita, J. G. Bednorz, and F. Lichtenberg, *Nature (London)* **372**, 532 (1994).

²M. Imada, A. Fujimori, and Y. Tokura, *Rev. Mod. Phys.* **70**, 1039 (1998).

³M. Salamon and M. Jaime, *Rev. Mod. Phys.* **73**, 583 (2001).

⁴S. N. Ruddlesden and P. Popper, *Acta Crystallogr.* **10**, 538 (1957).

⁵K. Ishida, H. Mukuda, Y. Kitaoka, K. Asayama, Z. Q. Mao, Y. Mori, and Y. Maeno, *Nature (London)* **396**, 658 (1998).

⁶K. D. Nelson, Z. Q. Mao, Y. Maeno, and Y. Liu, *Science* **306**, 1151 (2004).

⁷S. A. Grigera, R. S. Perry, A. J. Schofield, M. Chiao, S. R. Julian, G. G. Lonzarich, S. I. Ikeda, Y. Maeno, A. J. Millis, and A. P. Mackenzie, *Science* **294**, 329 (2001).

⁸R. A. Borzi, S. A. Grigera, J. Farrell, R. S. Perry, S. J. S. Lister, S. L. Lee, D. A. Tennant, Y. Maeno, and A. P. Mackenzie, *Science* **315**, 214 (2007).

⁹L. Klein, J. S. Dodge, C. H. Ahn, G. J. Snyder, T. H. Geballe, M. R. Beasley, and A. Kapitulnik, *Phys. Rev. Lett.* **77**, 2774 (1996).

¹⁰B. Allen, H. Berger, O. Chauvet, L. Forro, T. Jarlborg, A. Junod, B. Revaz, and G. Santi, *Phys. Rev. B* **53**, 4393 (1996).

¹¹G. Cao, S. McCall, M. Shepard, J. E. Crow, and R. P. Guertin, *Phys. Rev. B* **56**, 321 (1997).

¹²Y. Kata, L. Klein, J. W. Reiner, T. H. Geballe, M. R. Beasley, and A. Kapitulnik, *Phys. Rev. B* **63**, 054435 (2001).

¹³L. Pi, A. Maignan, R. Retoux, and B. Raveau, *J. Phys.: Condens. Matter* **14**, 7391 (2002).

¹⁴D. A. Crandles, M. M. Yazdani, and F. S. Razavi, *J. Phys. D: Appl. Phys.* **39**, 6 (2006).

¹⁵G. Cao, S. McCall, J. Bolivar, M. Shepard, F. Freibert, P. Henning, J. E. Crow, and T. Yuen, *Phys. Rev. B* **54**, 15144 (1996).

¹⁶S. L. Cuffini, V. A. Macagno, R. E. Carbonio, A. Melo, E. Trollund, and J. L. Gautier, *J. Solid State Chem.* **105**, 161 (1993).

¹⁷A. Maignan, C. Martin, M. Hervieu, and B. Raveau, *Solid State Commun.* **117**, 377 (2001).

¹⁸A. J. Williams, A. Gillies, J. P. Attfield, G. Heymann, H. Huppertz, M. J. Martínez-Lope, and J. A. Alonso, *Phys. Rev. B* **73**, 104409 (2006).

¹⁹C. Bansal, H. Kawanaka, R. Takahashi, and Y. Nishihara, *J. Alloys Cmps.* **360**, 47 (2003).

²⁰A. Mamchik and I.-W. Chen, *Phys. Rev. B* **70**, 104409 (2004).

²¹K. Nomura, R. Zboril, J. Tucek, W. Kosaka, S. Ohkoshi, and I. Felner, *J. Appl. Phys.* **102**, 013907 (2007).

²²J. Fan, L. Ling, B. Hong, L. Pi, and Y. Zhang, *J. Magn. Magn. Mater.* **321**, 2838 (2009).

²³M. W. Lufaso, P. W. Woodward, and J. Goldberger, *J. Solid State Chem.* **177**, 1651 (2004).

²⁴R. V. K. Mangalam and A. Sundaresan, *Mater. Res. Bull.* **44**, 576 (2009).

²⁵R. Nithya, V. Sankara Sarthy, P. Paul, T. C. Han, J. G. Lin, and F. C. Chou, *Solid State Commun.* **149**, 1674 (2009).

²⁶I. Felner, K. Nomura, and I. Nowik, *Phys. Rev. B* **73**, 064401 (2006).

²⁷Y. Ying, J. Fan, Z. Qu, B. Hong, S. Tan, and Y. Zhang, *Phys. Rev. B* **74**, 144433 (2006).

²⁸A. Chakravarti, R. Ranganathan, and C. Bansal, *Solid State Commun.* **82**, 591 (1992).

²⁹L. Klein, J. S. Dodge, C. H. Ahn, J. W. Reiner, L. Mieville, T. H. Geballe, M. R. Beasley, and A. Kapitulnik, *J. Phys.: Condens. Matter* **8**, 10111 (1996).